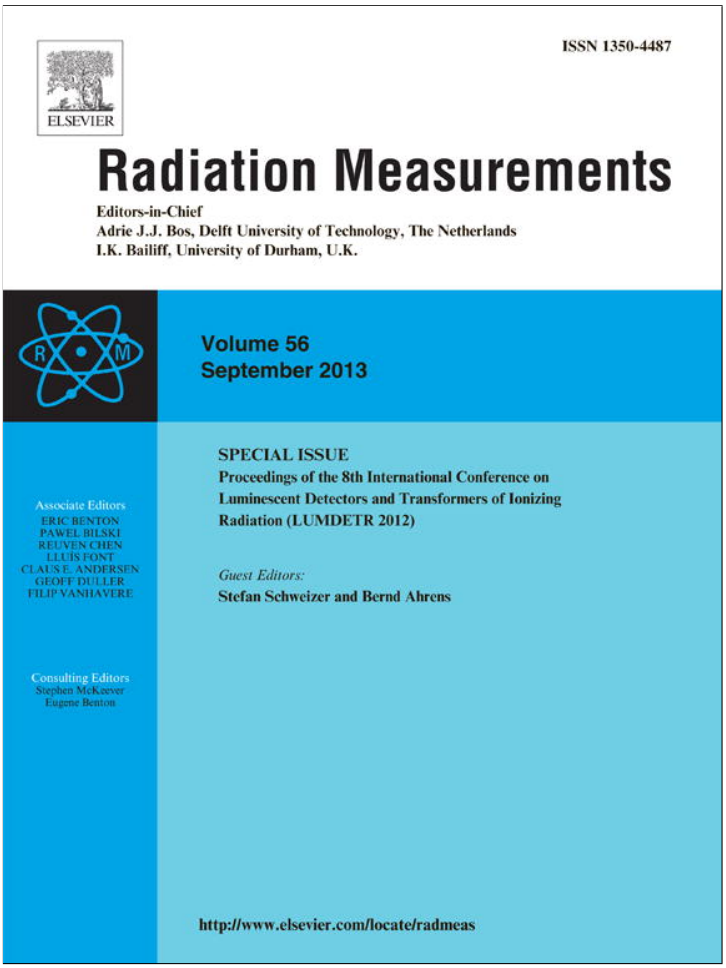

Radiation Measurements 56 (2013) 6–12

Contents lists available at SciVerse ScienceDirect

Radiation Measurements

journal homepage: www.elsevier.com/locate/radmeas

Modeling TL-like thermally assisted optically stimulated luminescence (TA-OSL)

R. Chen [a,*], V. Pagonis [b]

[a] Raymond and Beverly Sackler School of Physics and Astronomy, Tel-Aviv University, Haim Levanon St., Ramat-Aviv, Tel-Aviv 69978, Israel
[b] Physics Department, McDaniel College, Westminster, MD21157, USA

HIGHLIGHTS

- Thermally assisted optically stimulated luminescence (TA-OSL) theory.
- Simulation of TA-OSL at different stimulation intensities.
- Analysis of the TL-like TA-OSL curves.
- Determination of effective activation energies and frequency factors.
- Comparison of the numerical simulation results and the analytical expressions.

ARTICLE INFO

Article history:
Received 21 September 2012
Received in revised form
14 December 2012
Accepted 18 December 2012

Keywords:
Thermally assisted optically stimulated luminescence (TA-OSL)
Two-stage
Thermal stimulation
Simulation

ABSTRACT

In this work we present a model for thermally assisted optically stimulated luminescence (TA-OSL), an effect previously observed in experimental work. The model consists of one trapping state with an excited state beneath the conduction band and one kind of recombination center. In one version, we assume that an electron is thermally elevated to the excited state. From there it can either be raised optically into the conduction band or it can be de-excited back into the ground state of the trap. Once in the conduction band, the electron may retrap in the excited state or recombine with a hole in a center, yielding a luminescence photon. The other version is similar except that once the electron is in the excited state, it may be elevated to the conduction band either optically or thermally, with activation energy E_2 and frequency factor s_2. Using approximations along with analytical considerations as well as numerical simulations consisting of the solution of the simultaneous differential equations with linear heating function, the resulting TL-like curves are studied. First-order like and second-order like cases as well as intermediate cases are identified. The conditions for reaching these situations are considered; it is shown that they are not simply the same as in regular TL, and in addition to the trapping parameters, the intensity of the stimulating light also plays a role.

1. Introduction

In thermoluminescence (TL) and optically stimulated luminescence (OSL), a luminescent sample is first irradiated and the absorbed energy may be emitted later during heating in the former case and during light exposure in the latter. An effect of thermally assisted OSL (TA-OSL) has been reported in several materials, which is, in a sense, a combination of the two phenomena. It appears that Hütt et al. (1988) were the first to present this effect. They report on infra-red stimulated luminescence (IRSL) in feldspars. Using infrared wavelengths, direct excitation from the deep trap into the conduction band appears to be impossible, and thermal assistance has been shown to be crucial. Here, IR seems to elevate the electron into an excited state, from which it is thermally raised into the conduction band with an activation energy E. Measuring the OSL as a function of temperature may yield an estimated value of E. Further discussion of TA-IRSL of feldspars was given by Bailiff and Poolton (1991), Clark and Sanderson (1994) and Poolton et al. (1995). An alternative explanation to a similar effect in quartz stimulated by green light has been given by Spooner (1994). He considered the existence of an array of states within the ground state of the trap so that the upper level of the array is accessed at high temperature with an activation energy E. The optical energy required for stimulation is smaller than the depth of the bottom of the trap. Thus, the TA-OSL phenomenon is reached by raising electrons thermally into an excited state from which they are optically released into the conduction band. Duller and Wintle (1991) and Duller and Bøtter-Jensen (1993) reported on the effect

* Corresponding author. Tel.: +972 3 6408426; fax: +972 9 9561213.
E-mail address: chenr@tau.ac.il (R. Chen).

1350-4487/$ – see front matter © 2013 Elsevier Ltd. All rights reserved.
http://dx.doi.org/10.1016/j.radmeas.2012.12.021

in potassium feldspar samples, and were the first to present a TL-like TA-OSL. Here, following irradiation, the sample was IR illuminated and, simultaneously heated using constant heating rate. The results of TA-OSL and TL in the same samples were compared and the maximum of the former occurred at a lower temperature than that of the latter. Poolton et al. (1994) explained the effect of TA-OSL by a donor-acceptor (D-a) model. As explained by these authors, excitation into an excited state leads to the overlap of the excited-state wavefunctions, and a thermally assisted hopping, with activation energy E leading to radiative recombination takes place. Markey et al. (1995, 1996) report on TA-OSL in α-Al_2O_3:C and also show a TL-like peak which occurs at a lower temperature than its counterpart TL peak. They give a model which includes shallow traps, dosimetric traps, deep traps and recombination centers, and simulate the curves of TA-OSL under these circumstances. More work on TA-OSL of Al_2O_3:C has been reported by Akselrod et al. (1998). Also discussed TA-OSL in Al_2O_3:C Polymeris et al. (2010) and Mishra et al. (2011). The latter authors presented TL-like curves and tried to explain them using the Spooner two-stage model in which the first stage is thermal and the second is optical. They then assumed that the thermal stage is either of first order or of general order, and developed expressions for the TL-like peaks. A review paper by McKeever et al. (1997) sums up the experimental results and some theoretical aspects of TA-OSL. Some more evidence of this phenomenon in different materials includes the papers by Bandyopadhyay et al. (1999) on TA-OSL in KCl:Cu, Fattahi (2009) in K-rich feldspar and Dotzler et al. (2009) in $RbMgF_3:Eu^{2+}$. Thermally assisted OSL in quartz has been discussed in the comprehensive papers on quartz luminescence by Smith and Rhodes (1994), Bailey (2001) and by Jain et al. (2005). Kitis et al. (2010) and Chruścińska and Przegiętka (2010) also discussed TA-OSL in quartz. The latter explain the effect in terms of the optical cross section (OCS) dependence on temperature. A recent work by McKeever et al. (2010) mentions the occurrence of TA-OSL in Martian sediments. Finally, Chen et al. (2012) have discussed a two-stage stimulation of thermoluminescence which seems to have similarities to TA-OSL. While dealing with this rather complex situation, these authors defined the effective activation energy and the effective frequency factor, namely the values that one gets by using the standard methods for glow-curve analysis. Using simulations as well as analytical treatment, it has been shown that in most cases, the effective activation energy is the sum of the energies of the two stages. However, cases in which the effective activation energy E_{eff} is close to E_1, the energy of the first stage, have been identified. On the basis of these cases, an effect of anomalous stability has been predicted. A paper by Oster and Haddad (2003) on "thermo-photo stimulated electron emission" bears interesting resemblance to TA-OSL. Here, three peaks of thermally stimulated electron emission (TSEE) are enhanced by additional illumination.

In the present work we deal with the features of TL-like TA-OSL curves based on the simultaneous differential equations governing the two-stage process using both numerical simulations and analytical considerations. Cases where the second stage consists of optical stimulation are discussed, with thermal stimulation being active for one of the stages or both. By using the shape of the peak and temperature of maximum luminescence intensity, the effective activation energy and frequency factor are obtained, and are compared with their values inserted in the model. Also, the role of the stimulation coefficient $f(s^{-1})$ and its relative effect to the frequency factor $s(s^{-1})$ in producing the effective frequency factor s_{eff} is studied.

2. The models

The two-stage energy band model associated with the process suggested by Spooner (1994) is shown in Fig. 1. The trapping state

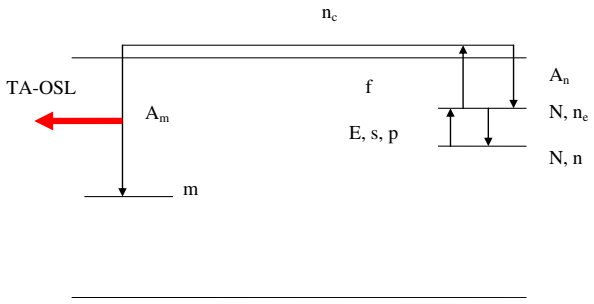

Fig. 1. Energy level diagram of the TA-OSL model. Here, the first stage of electron elevation is thermal and the second stage is optical.

with concentration $N(\mathrm{cm}^{-3})$ and instantaneous occupancy $n(\mathrm{cm}^{-3})$ are shown along with the excited state $n_e(\mathrm{cm}^{-3})$. The activation energy for the thermal elevation into the excited state is $E(\mathrm{eV})$ and the frequency factor is $s(\mathrm{s}^{-1})$. Once the electron is in the excited state, it can either retrap with a probability of $p(\mathrm{s}^{-1})$ or be optically excited into the conduction band. The probability for this transition $f(\mathrm{s}^{-1})$ is proportional to the intensity of the stimulating light and to the optical cross section of the trap. The instantaneous concentration of electrons in the conduction band is denoted by $n_c(\mathrm{cm}^{-3})$. From the conduction band, the electrons can be retrapped into the excited state with a retrapping probability coefficient of $A_n(\mathrm{cm}^3\mathrm{s}^{-1})$, or recombine with a hole in the center with a probability coefficient of $A_m(\mathrm{cm}^3\mathrm{s}^{-1})$. This recombination is assumed to produce the TL photons with an instantaneous intensity I. The emitted light is shown by the thick arrow. At the end of the initial excitation by irradiation, the number of trapped holes, m_0, is equal to the total number of trapped electrons, namely, $n_0 + n_{e0} + n_{c0}$, however, since the excitation is performed at a relatively low temperature, n_{e0} and n_{c0} can be considered to be relatively small so that $n_0 \approx m_0$. The recombination of the electron from the conduction band with the hole in the center is assumed to produce a photon. In accordance with the detailed-balance principle and neglecting electronic degeneracies, the values of the frequency factor for the first transition, s, and the retrapping probability, p, must, according to Halperin and Braner (1960), be equal: $s = p$.

The coupled differential equations governing the process during the heating stage, shown in Fig. 1 are

$$\frac{dn}{dt} = -sn\exp(-E/kT) + pn_e, \tag{1}$$

$$\frac{dn_e}{dt} = A_n(N - n - n_e)n_c + sn\exp(-E/kT) - fn_e - pn_e, \tag{2}$$

$$I = -\frac{dm}{dt} = A_m m n_c, \tag{3}$$

$$\frac{dn_c}{dt} = \frac{dm}{dt} - \frac{dn}{dt} - \frac{dn_e}{dt}. \tag{4}$$

As suggested by Chen et al. (2012), in writing the first term on the right-hand side of Eq. (2) one assumes that no retrapping into the excited state n_e is possible if there is an electron either in the ground state of the trap or in its excited state. Simulation of the TL-like TA-OSL curve is reached by choosing an appropriate set of parameters and solving numerically Eqs. (1)–(4) with a certain heating function, usually linear.

An alternative model has to do with the scheme suggested by Hütt et al. (1988), namely that the first stage is optical and the

second is thermal. The set of coupled equations should be amended and Eqs. (1) and (2) should be replaced by

$$\frac{dn}{dt} = -fn + pn_e, \tag{5}$$

$$\frac{dn_e}{dt} = fn - pn_e + A_n(N-n-n_e)n_c - sn_e\exp(-E/kT). \tag{6}$$

Note that E and s here are associated with the thermal transition from the localized excited state into the conduction band. In order to follow the TA-OSL here, one should solve Eqs. (3)–(6) with a certain heating function. Note also that in this case, s and p are independent parameters since they are not associated with the same transition; s is the frequency factor for the second stage whereas p is associated with retrapping in the first stage. Thus, the system has one-more free parameter which makes the analysis of the results in terms of effective values of s and A_n more complicated (see section 3 below). Moreover, from the experimental point of view, in order that an optical elevation between a localized state and its excited state be possible, photons of the exact energy are required. Such a condition is not easily achieved experimentally although, apparently, this is the case with IR stimulation in feldspars mentioned above. Anyway, this is not the case if the second stage is optical since the transition into the conduction band is not restricted by an exact energy in this case. Due to these reasons, we concentrate here on the mentioned Spooner model as shown in Fig. 1.

One can also think about the possibility that in both stages electrons can be thermally stimulated, but the second stage is also light sensitive. This may be the case where TL is measurable with no light stimulation, by the two-stage thermal transition (Chen et al., 2012), but it is enhanced by the stimulating light as appears to be the case in some of the mentioned references (e.g. Duller and Wintle, 1991; Mishra et al., 2011). One should consider now E_1 and s_1 associated with the first stage and E_2 and s_2 related to the second stage. Eqs. (1) and (2) should be replaced now by

$$\frac{dn}{dt} = -s_1 n\exp(-E_1/kT) + pn_e. \tag{7}$$

$$\frac{dn_e}{dt} = A_n(N-n-n_e)n_c + s_1 n\exp(-E_1/kT) - fn_e - pn_e - s_2 n_e\exp(-E_2/kT). \tag{8}$$

Note that as explained above, here too $s_1 = p$ due to the detailed-balance principle. The combined TL, TA-OSL curve can be simulated here by solving numerically the set of Eqs. (3), (4), (7) and (8) with some heating function.

One could also consider the case where both stages are possible thermally and the first stage is optically sensitive as well as the case where both stages are thermally and optically sensitive and the appropriate equations can be written and solved. If the latter case is pursued, for a given light exposure two stimulation factors, f_1 and f_2 are to be considered since the electron elevation in the two stages may have different sensitivities to light.

3. Analytical considerations

Let us consider Eq. (2) which is one of the set of equations governing the situation in which the first stage is thermal and the second is optical, and apply the quasi-equilibrium condition which in this case can be written as

$$\frac{dn_e}{dt} << (p+f)n_e. \tag{9}$$

Using this condition with Eq. (2) yields

$$n_e = \frac{A_n(N-n-n_e)n_c + ns\exp(-E/kT)}{p+f}. \tag{10}$$

Consistently with the quasi-equilibrium assumptions we can write $n_e << (N-n)$, which can be expected as long as the trap is not in full saturation. Substituting Eq. (10) into Eq. (1) yields

$$\frac{dn}{dt} = p\frac{A_n(N-n)n_c + ns\exp(-E/kT)}{p+f} - s\exp(-E/kT)n. \tag{11}$$

Rearranging Eq. (11) changes this formula into

$$\frac{dn}{dt} = -ns_{\text{eff}}\exp(-E/kT) + A_{n,\text{eff}}(N-n)n_c, \tag{12}$$

where

$$s_{\text{eff}} = \frac{sf}{p+f} = \frac{pf}{p+f}, \tag{13}$$

and

$$A_{n,\text{eff}} = \frac{p}{p+f}A_n. \tag{14}$$

In getting Eq. (13) we used the mentioned detailed-balance principle, which states here that $s = p$. Eq. (12) looks exactly like the conventional one-stage expression for TL in the one-trap one-recombination-center model (OTOR), but with the effective rate constants s_{eff} and $A_{n,\text{eff}}$ given in Eqs. (13) and (14). We can amend Eq. (4) to read approximately

$$\frac{dn_c}{dt} = \frac{dm}{dt} - \frac{dn}{dt}. \tag{15}$$

Thus, the set of Eqs. (3), (12) and (15) is in full analogy to the equations governing the regular one-trap one-recombination-center (OTOR) set with single stage thermal stimulation (see e.g. Chen et al., 2009) as applied to TL. Note that according to Eq. (13), if $f << p$, then $s_{\text{eff}} \approx f$ whereas if $p << f$, then $s_{\text{eff}} \approx p$. As for Eq. (14), if $f << p$ then $A_{n,\text{eff}} \approx A_n$ and if $p << f$ then $A_{n,\text{eff}} = (p/f)A_n$. The previously discussed (see e.g. Chen and Pagonis (2011), pp. 42, 43) conditions between the recombination probability coefficient A_m and retrapping probability coefficient A_n leading to first-, second- and intermediate-order kinetics should include in the present case $A_{n,\text{eff}}$. The main new point here is that this magnitude depends on f which is proportional to the stimulating light intensity. This is a rather unusual effect, in which the apparent kinetics of the TA-OSL process seems to depend on the intensity of the stimulating light.

Some change in these results can be seen in the case where the second stage is both thermal and optical. Starting from Eq. (8) and making the same quasi-equilibrium assumptions as before, we get instead of Eq. (11)

$$\frac{dn}{dt} = p\frac{A_n(N-n)n_c + ns_1\exp(-E_1/kT)}{p+f+s_2\exp(-E_2/kT)} - s_1\exp(-E_1/kT)n. \tag{16}$$

This can also be reduced to the form of Eq. (12), with E_1 replacing E, namely,

$$\frac{dn}{dt} = -ns_{\text{eff}}\exp(-E_1/kT) + A_{n,\text{eff}}(N-n)n_c, \tag{17}$$

but with different expressions for s_{eff} and $A_{n,\text{eff}}$, namely,

$$s_{\text{eff}} = p\frac{f + s_2\exp(-E_2/kT)}{p + f + s_2\exp(-E_2/kT)}, \quad (18)$$

and

$$A_{n,\text{eff}} = \frac{pA_n}{p + f + s_2\exp(-E_2/kT)}. \quad (19)$$

As pointed out by Chen et al. (2012), in the case of two-stage thermal excitation, which is the same as the present case but with $f = 0$, the relation between p and $s_2\exp(-E_2/kT)$ determines the nature of the TL peak. In that case, $s_2 exp(-E_2/kT) << p$ resulted in $s_{\text{eff}} = s_2$ and $A_{n,\text{eff}} = A_n$ and the effective activation energy was $E_1 + E_2$; this situation in the model previously predicted an effect of anomalous stability of the TL signal. The opposite condition of $s_2 exp(-E_2/kT) >> p$ yields $s_{\text{eff}} = s_1 exp(E_2/kT)$ and $A_{n,\text{eff}} = (p/s_2) exp(E_2/kT) A_n$. As described by Chen et al. (2012), the effective energy may reduce there to E_1 and the effective frequency factor to s_1. In the present case of TL-like TA-OSL, the comparison determining the exact behavior has to do with the relation between $f + p$ and $s_2\exp(-E_2/kT)$, which obviously means that the effective values may depend on the stimulation intensity f.

4. Numerical results

The set of simultaneous Eqs. (1)–(4) was solved numerically for chosen sets of the trapping parameters and the simulating light intensity factor f, with a certain linear heating function $T = T_0 + \beta t$, using the ode15s MATLAB solver. The heating rate β was always chosen to be 1 K/s.

The set of parameters used for Fig. 2 are: $E = 0.5$ eV; $p = s = 10^{10}$ s^{-1}; $N = 1.1 \times 10^{10}$cm^{-3}; $n_0 = m_0 = 10^{10}$cm^{-3}; $n_{e0} = 0$; $A_m = 10^{-7}$cm^{3}s^{-1}; $A_n = 10^{-12}$cm^{3}s^{-1}. As could be expected from the large recombination probability coefficient, 5 orders of magnitude larger than the retrapping probability coefficient, the peak symmetry in all these peaks is close to typical first-order TL peaks, namely $\mu_g \approx 0.44$, where $\mu_g = \delta/\omega$, where $\delta = T_2 - T_m$; $\omega = T_2 - T_1$ and where T_m is the temperature at the maximum and T_1, T_2 are the low and high temperatures of half intensity, respectively (see e.g., Chen, 1969). The effective activation energies have been determined by the equation

$$E_{\text{eff}} = 2.52\frac{kT_m^2}{\omega} - 2kT_m, \quad (20)$$

and the effective frequency factor has been found from the maximum condition (see e.g., Chen, 1969)

$$s_{\text{eff}} = \frac{\beta E}{kT_m^2}\exp(E/kT_m). \quad (21)$$

The curves shown in Fig. 2 are with different values of the stimulating light intensity, f. In curve (a) it is $f = 10^5$ s^{-1}; in (b), $f = 10^7$ s^{-1}; in (c), $f = 10^9$ s^{-1} and in (d, e), two nearly coincident peaks for $f = 10^{11}$ s^{-1} and 10^{13} s^{-1}, respectively. Using Eq. (20), we get for all the peaks shown in Fig. 2, $E_{\text{eff}} \sim 0.5$ eV. The reason for their occurrence at different temperature has to do with different values of s_{eff}. Using Eq. (21) we get the effective values of the frequency factor which are: (a) $s_{\text{eff}} \sim 10^5$ s^{-1}; (b) $s_{\text{eff}} \sim 10^7$ s^{-1}; (c) $s_{\text{eff}} \sim 10^9$ s^{-1}; (d, e) $s_{\text{eff}} \sim 10^{10}$ s^{-1}. As can be seen, the peaks (d) and (e) nearly coincide. Note that in another result, not shown here, the used value of f was 10^{10} s^{-1}, and the peak occurred between (c) and (d, e). Using Eq. (21) yielded $s_{\text{eff}} \sim 5 \times 10^9$ s^{-1}. These results of the effective frequency factors are in very good agreement with Eq. (13). As long as $f << p$, we have $s_{\text{eff}} \sim f$ whereas when $f >> p$, $s_{\text{eff}} \sim$ p. This is the reason why curves (d) and (e) nearly coincide. Although there is a difference of two orders of magnitude in f, since it is significantly higher than p, the effective frequency factor is nearly equal to p and the peak occurs at nearly the same temperature. As for the case where $f = p$, the curve still looks like first-order peak occurring between curves (c) and (d), with an effective frequency factor of $\sim 5 \times 10^9$ s^{-1} as is expected from Eq. (13) for this case.

In another set of simulations the results of which shown in Fig. 3, we depict the opposite case where retrapping is significantly higher than recombination. Here we have used $A_m = 10^{-10}$ cm^{3}s^{-1} and $A_n = 10^{-5}$ cm^{3}s^{-1}. Like in the previous case, curves (a–e) correspond to values of the stimulating light intensity f of 10^5, 10^7, 10^9, 10^{11} and 10^{13} s^{-1}, respectively. The peaks here look more

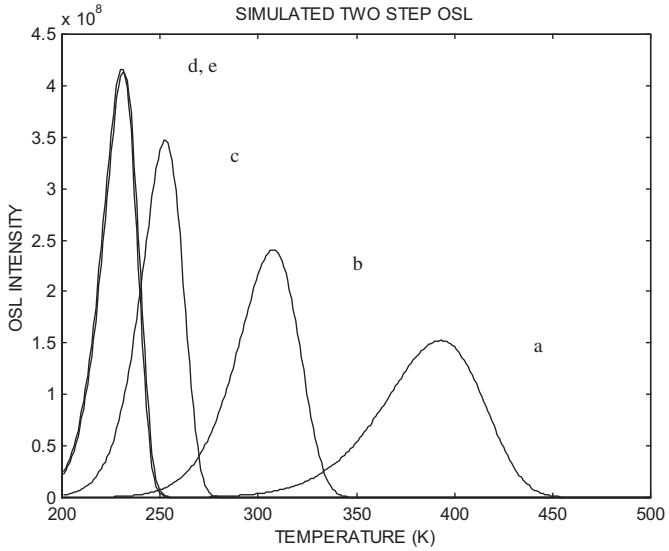

Fig. 2. TL-like TA-OSL curves simulated using Eqs. (1)–(4) for different values of f, the stimulating light intensity factor. The trapping parameters given in the text are such that the peaks look approximately like first-order TL curves. (a) $f = 10^5$ s^{-1}. (b) $f = 10^7$ s^{-1}. (c) $f = 10^9$ s^{-1}. (d) $f = 10^{11}$ s^{-1}. (e) $f = 10^{13}$ s^{-1}.

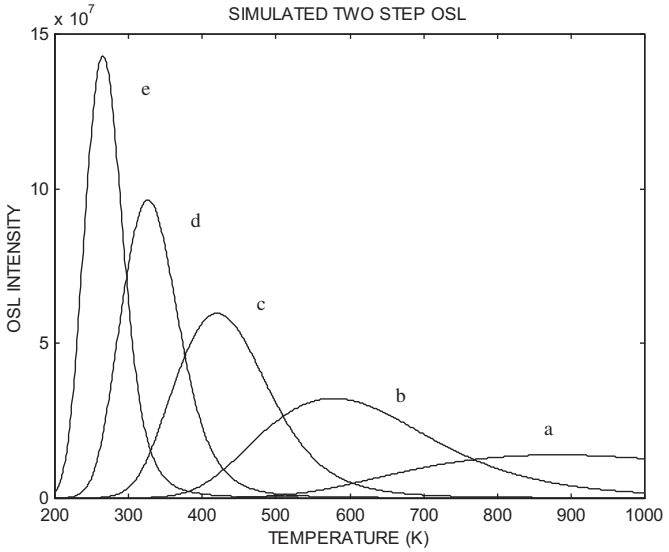

Fig. 3. TL-like TA-OSL curves simulated using Eqs. (1)–(4) for different values of f, the stimulating light intensity factor. The trapping parameters given in the text are such that the peaks look approximately like second-order TL curves. (a) $f = 10^5$ s^{-1}. (b) $f = 10^7$ s^{-1}. (c) $f = 10^9$ s^{-1}.(d) $f = 10^{11}$ s^{-1}. (e) $f = 10^{13}$ s^{-1}.

like conventional second-order curves with $\mu_g \approx 0.54$. Here too, the peak occurs at a higher temperature for lower values of f though the meaning of s_{eff} is not as clear as in the first-order case.

The results of a third set of simulations which are intermediate in a sense, is shown in Fig. 4. Here we chose $A_m = 10^{-8}$ cm^{3}s^{-1} and $A_n = 10^{-6}$ cm^{3}s^{-1}. The values of f in curves (a–e) are the same as in the previous cases. It seems obvious that the symmetry in curves (a) and (b) is typical of second-order peaks whereas in (d) and (e) it is like first order. The symmetry of curve (c) is intermediate. The transition from first- to second-order shape can be understood with the aid of Eq. (14). As long as $p >> f$, we see that $A_{n,\text{eff}} \sim A_n$. This is the case in curves (a) and (b), and since $A_n > A_m$, approximately second order results. In curves (d) and (e), $f > p$, and since f is larger, $A_{n,\text{eff}}$ gets smaller and therefore the shift is toward the first-order shape.

Fig. 5 depicts the results of simulations of the same model in the case where the second stage consists of both thermal and optical stimulation. The parameters are the same as in Fig. 2, but E and s are now denoted E_1, s_1 for the first stage and the activation energy and frequency factor of the second stage are denoted E_2, s_2, respectively and their values are taken as 0.4eV and 10^{10} s^{-1}. Curves (b–e) for f values of 10^7, 10^9, 10^{11} and 10^{13} s^{-1} are practically the same as in Fig. 2. The peaks look like first-order peaks and the activation energy evaluated from curves (b–e) is 0.5 eV like before. Curve (f) is found with $f = 0$, namely, this is a double-stage TL peak. This peak also looks like a first-order curve. Using Eq. (20) we get $E_{\text{eff}} \sim 0.9$ eV and $s_{\text{eff}} \sim 10^{10}$ s^{-1}. In view of the results by Chen et al. (2012), this could be expected. In the two-stage TL, in most cases, $E_{\text{eff}} \approx E_1 + E_2$, and $s_{\text{eff}} \approx s_2$ which agrees with the present results. Curve (a) of Fig. 5 differs from curve (a) in Fig. 2. In a sense it is intermediate between two-stage thermal curve (f) and two-stage thermal–optical curves (b–e). This peak also looks like being of first order, but the effective activation energy derived from Eq. (20) is 0.6 eV, which is intermediate between the values of 0.9 eV for $f = 0$ and 0.5 eV for the high values of f.

Fig. 6 shows the simulation results of the same model as in Fig. 5, namely, that both stages are stimulated thermally and the second stage is also stimulated optically. The parameters chosen are the same as in Fig. 3, namely with relatively high retrapping probability

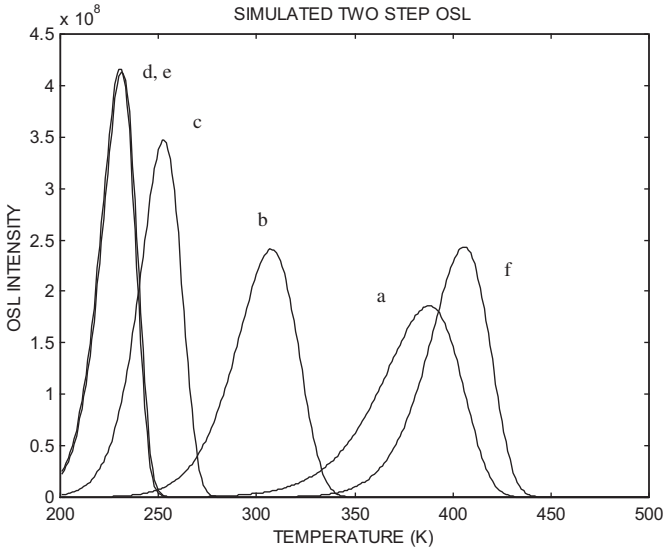

Fig. 5. TL-like curves of the combined TL-OSL, simulated by solving numerically Eqs. (3), (4), (7) and (8). The trapping parameters are similar to those in Fig. 2, except that in addition to the optical stimulation of the second stage, thermal stimulation is also allowed. The stimulating light intensity coefficients f are: (a) $f = 10^5$ s^{-1}. (b) $f = 10^7$ s^{-1}. (c) $f = 10^9$ s^{-1}. (d) $f = 10^{11}$ s^{-1}. (e) $f = 10^{13}$ s^{-1}. (f) $f = 0$.

coefficient. Here, $A_n = 10^{-5}$ cm^{3}s^{-1} and $A_m = 10^{-10}$ cm^{3}s^{-1}. The peaks shown are for (a) $f = 10^5$ s^{-1}; (b) $f = 10^7$ s^{-1}; (c) $f = 10^9$ s^{-1}; (d) $f = 10^{11}$ s^{-1}; (e) $f = 10^{13}$ s^{-1}. All the peaks appear to have approximately second-order symmetry. Curves (c, d, e) are practically the same as those in Fig. 3. The effect of the thermal stimulation of the second stage is seen mainly in the shape of curves (a) in the two figures, and to a smaller extent, in Curves (b).

One more possible variation of the model has been considered. Similarly to the two cases in Figs. 5 and 6, we allow for thermal stimulation of the two stages but assume that the optical stimulation is from the ground state into the conduction band. Strictly speaking, this is not thermally assisted OSL since the electrons are raised into the conduction band either thermally, in two stages, or

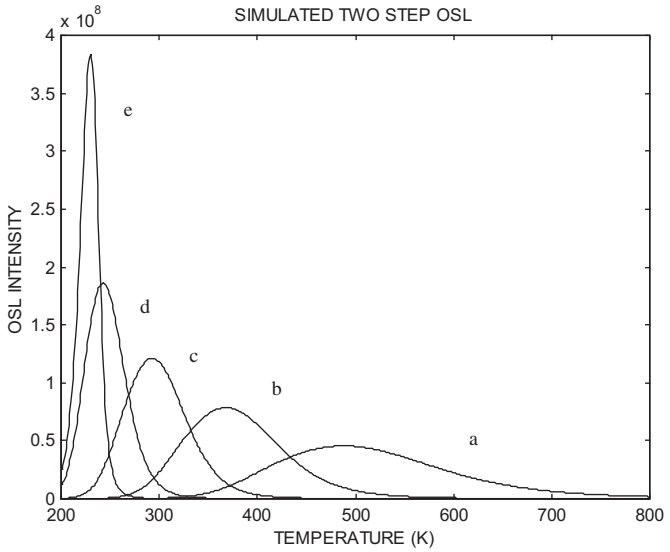

Fig. 4. TL-like TA-OSL curves simulated using Eqs. (1)–(4) for different values of f, the stimulating light intensity factor. The trapping parameters given in the text are such that for low values of f, the peaks look like second-order TL curves, but for higher values, the shape changes to that of first order. (a) $f = 10^5$ s^{-1}. (b) $f = 10^7$ s^{-1}. (c) $f = 10^9$ s^{-1}. (d) $f = 10^{11}$ s^{-1}. (e) $f = 10^{13}$ s^{-1}.

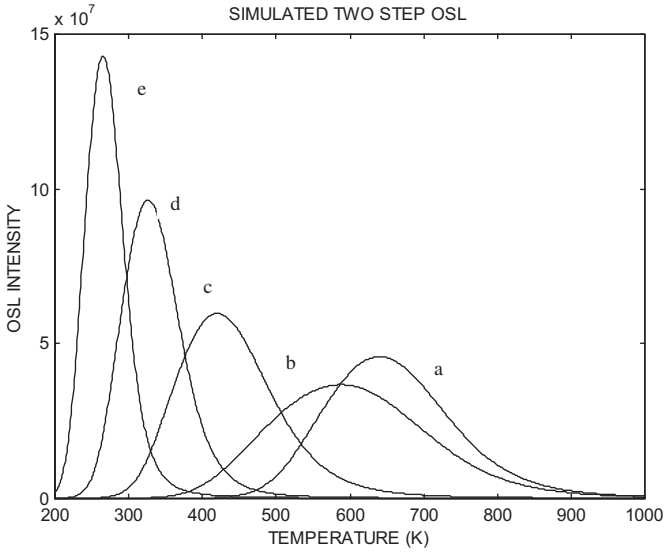

Fig. 6. TL-like curves of the combined TL-OSL, simulated by solving numerically Eqs. (3), (4), (7) and (8). The trapping parameters are similar to those in Fig. 3, except that in addition to the optical stimulation of the second stage, thermal stimulation is also allowed. The stimulating light intensity coefficients f are: (a) $f = 10^5$ s^{-1}. (b) $f = 10^7$ s^{-1}. (c) $f = 10^9$ s^{-1}. (d) $f = 10^{11}$ s^{-1}. (e) $f = 10^{13}$ s^{-1}.

optically. However, since the measured luminescence is a result of both heating and illumination, from the experimental point of view, it is the same as TA-OSL. The governing equations here will be

$$\frac{dn}{dt} = -s_1 n\exp(-E_1/kT) + pn_e - fn, \tag{22}$$

$$\frac{dn_e}{dt} = A_n(N-n-n_e)n_c + s_1 n\exp(-E_1/kT) - pn_e - s_2 n_e\exp(-E_2/kT). \tag{23}$$

The set of equations to be solved for this case is (3, 4, 22, 23). An example of the numerical results is shown in curve (a) of Fig. 7. The results are found with the same set of parameters as in Fig. 5, and with $f = 0.01\ s^{-1}$. Note that a significantly smaller value of f is required here than in the previous cases because the optical elevation here is from the ground state (n) and not from the excited state (n_e). Since n is significantly larger than n_e, much smaller values of f are required for the optical stimulation. The decay of OSL is dominating in the range between 200 and ~350 K, but then the TL component can be seen with a maximum at ~400 K. For comparison, we repeated the simulation with $f = 0$, namely, the two-stage excited TL (see Chen et al., 2012), the result is shown in curve (b). These results are in very good qualitative agreement with the experimental results of Mishra et al. (2011) as shown in curves (A) and (C) of their Fig. 5.

5. Discussion

In this work, we studied two models, previously mentioned in the literature, of thermally assisted OSL (TA-OSL) and described some results of numerical simulation with some sample sets of chosen trapping parameters. The relevant sets of coupled rate equations are written for these cases. In both cases, we follow the expected results both by approximations along with analytical treatment and by numerical solution of the sets of differential equations for certain representative sets of trapping parameters.

Both models consist of a trapping level from which electrons are first stimulated thermally into an excited state. As for the second stage of excitation from this excited state into the conduction band, in the first model it is done only optically whereas in the second model, electrons can be raised to the conduction band both thermally and optically. From the conduction band, they may either recombine with trapped holes in the luminescence center, yielding luminescence emission or retrap into the excited trapping level.

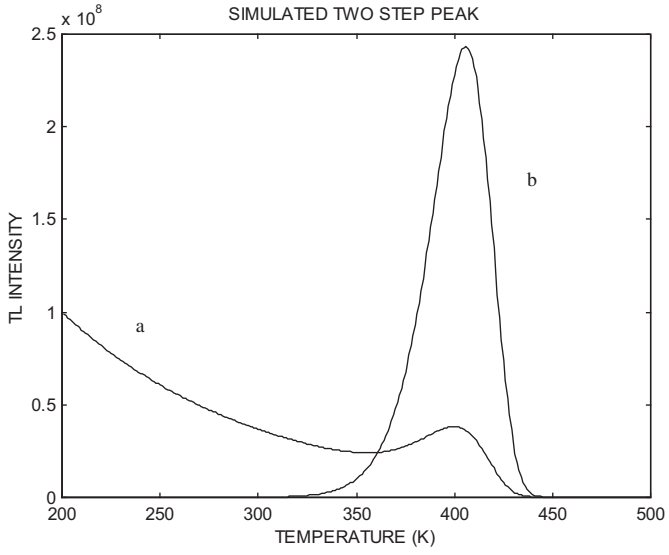

Fig. 7. With the same parameters as in Fig. 5, and with $f = 0.01\ s^{-1}$, curve (a) depicts the combined TL, OSL found by solving numerically Eqs. (3), (4), (22) and (23). Curve (b) is the double-stage TL found with the same parameters but with $f = 0$.

The numerical results depict the behavior of TA-OSL curves which look approximately like regular TL peaks. For the case of only optical stimulation during the second stage, an approximate effective set of Eqs. (3), (12) and (15) can explain the basic numerical results. The set is entirely analogous to the equations governing the well-known OTOR TL situation, but with effective values of s and A_n as given in Eqs. (13) and (14), respectively. Since $A_{n,\mathrm{eff}}$ depends on the relation between the probability p and the stimulating light intensity f, the transition between first- and second-order kinetics differs in the present case from the OTOR TL situation. Anyway, the parameters are chosen for Fig. 2 such that all the peaks have first-order kinetics. The effective activation energy determined by Eq. (20) is ~0.5 eV which is the inserted value. The effective frequency factor as found by Eq. (21) varies in the expected way as discussed above. As long as the stimulating light intensity factor f is smaller than s, $s_{\mathrm{eff}} \sim f$ and therefore it varies from curve (a) to (c) in Fig. 2. The peak occurs at lower temperature for higher values of f since this means that $s_{\mathrm{eff}} \sim f$ is larger. However, when f is larger than s, $s_{\mathrm{eff}} \sim s$ and therefore s_{eff} does not increase further for larger values of f, and the peak does not shift further for larger f. Note that the shift of the peak's temperature with the intensity of the stimulating lights as seen in curves (a) to (c) of Fig. 2 is compatible with the experimental results reported by Mishra et al. (2011) in α-Al_2O_3:C (see e.g. their Fig. 6). The shift also resembles qualitatively to their numerical results although their model is based on the heuristic "general-order" kinetics. Note also that peaks of TSEE have been reported (Oster and Haddad, 2003) to shift to lower temperatures by thermal activation in an effect which somewhat resembles the effect in TA-OSL described here.

One might expect that the amount of emitted light would increase with the intensity of the stimulation light. This is not so since, within the limits of this relatively simple model, it is quite obvious that the area under each curve is equal (if the appropriate units are considered) to the initial concentration in traps and centers n_0. Since this magnitude is the same in all the simulations, say in Fig. 2, the areas under the different curves are the same. From Eq. (20) it is evident that for two peaks with the same E_{eff}, if the maximum temperature T_m is smaller, the half width ω must be smaller as well. Since the areas of the different peaks remain the same, the narrower peaks must be higher, which indeed is clearly seen in Fig. 2. Qualitatively, the situation with the second-order peaks in Fig. (3) and with the transition situations in Fig. (4) is the same but here the explanation is not straightforward since the exact meaning of s_{eff} is not obvious in the non-first-order cases.

It should be noted that the condition for a peak to be of first order, second order and have intermediate kinetics does not depend only on the relation between the retrapping and recombination probability coefficients $A_{n,\mathrm{eff}}$ and A_m. This condition has to do with the relation between variable magnitudes rather than between constant parameters. In full analogy with the situation in regular OTOR TL peak (see e.g. Chen and Pagonis, 2011), one can say that the condition for getting a first-order peak is $A_m m >> A_{n,\mathrm{eff}}(N-n)$, along with $m \approx n$. The condition for second-order kinetics is $A_m m << A_{n,\mathrm{eff}}(N-n)$ along with $m \approx n$ and $N >> n$. The situation we are dealing with here is such that $m \approx n$ always takes place. Since both m and n are decreasing along the TA-OSL peak, if the latter condition leading to second order holds at the low temperature end of the peak, the inequality even becomes stronger when the temperature increases. On the other hand, if the former condition leading to first order occurs, it may be inverted at higher

temperatures when m and n decrease. Therefore, when we wanted to demonstrate the first-order behavior, we chose the parameters in such a way that A_m was significantly larger than $A_{n,\mathrm{eff}}$.

As pointed out above, the curves in Figs. 5 and 6 are associated with the model in which the first stage is thermal whereas the second stage is simultaneously thermal and optical. For large values of f, curves (b–e) in Fig. 5 and curves (c–e) in Fig. 6, the optical stimulation of the second stage dominates, and therefore, the curves are very similar to their corresponding ones in Figs. 2 and 3. Curve (f) in Fig. 5 represents the purely thermal two-stage stimulation, and as stated before (Chen et al., 2012), the effective value of the activation energy is $\sim E_1 + E_2 = 0.9$ eV. As can be seen from Eq. (20), large value of E_{eff} is associated with a narrower peak and this, in turn, is associated with a higher peak since the area under it is kept constant. Curve (a) with $f = 10^5\ \mathrm{s}^{-1}$ is intermediate between the large and nil values of f, and this results in the intermediate $E_{\mathrm{eff}} = 0.6$ eV. The situation in Fig. 6 is along the same lines but more complicated since the behavior is farther from being of first-order kinetics. The maximum intensity of peak (a) is larger than in peak (b) apparently since for $f = 10^5\ \mathrm{s}^{-1}$, the thermal stimulation of the first stage is dominant as compared to the optical elevation, hence the similarity to the relation between curves (f) and (a) in Fig. 5.

As for the case shown in Fig. 7, the combined optical-thermal effect is shown in curve (a) and compared to the thermal two-stage TL in curve (b). The fact that the maximum of the latter is significantly stronger than that of the former, has to do with the requirement that the area under the two curves must be the same. Since in the case of curve (a) many photons are emitted at the low-temperature range, the emission shown in curve (b) in the range of 330–440 K is significantly stronger. As pointed out above, the resemblance of these simulation curves to the experimental results by Mishra et al. (2011) (curves (A) and (C) in their Fig. 5) is quite remarkable.

References

Akselrod, M.S., Lucas, A.C., Polf, J.C., McKeever, S.W.S., 1998. Optically stimulated luminescence of Al_2O_3. Radiat. Meas. 29, 391–399.

Bailey, R.M., 2001. Towards a general kinetic model for optically and thermally stimulated luminescence of quartz. Radiat. Meas. 33, 17–45.

Bailiff, I.K., Poolton, N.R.J., 1991. Studies of charge transfer mechanisms in feldspars. Nucl. Tracks Radiat. Meas. 18, 111–118.

Bandyopadhyay, P.K., Russel, G.W., Chakrabarti, K., 1999. Optically stimulated luminescence in KCl:Cu X-irradiated at room temperature. Radiat. Meas. 30, 51–57.

Chen, R., 1969. On the calculation of activation energies and frequency factors from glow curves. J. Appl. Phys. 40, 570–585.

Chen, R., Pagonis, V., Lawless, J.L., 2009. A new look at the linear-modulated optically stimulated luminescence (LM-OSL) as a tool for dating and dosimetry. Radiat. Meas. 44, 344–350.

Chen, R., Pagonis, V., 2011. Thermally and Optically Stimulated Luminescence: A Simulation Approach. Wiley, Chichester.

Chen, R., Lawless, J.L., Pagonis, V., 2012. Two-stage thermal stimulation of thermoluminescence. Radiat. Meas. 47, 870–876.

Chruścińska, A., Przegiętka, K.R., 2010. The influence of electron-phonon interaction on the OSL decay curve shape. Radiat. Meas. 45, 317–319.

Clark, R.J., Sanderson, D.C.W., 1994. Photostimulated luminescence excitation spectroscopy of feldspars and micas. Radiat. Meas. 23, 641–646.

Dotzler, C., Williams, G.V.N., Rieser, U., Robinson, J., 2009. Photoluminescence, optically stimulated luminescence and thermoluminescence study of $RbMgF_3$:Eu^{2+}. J. Appl. Phys. 105, 023107.

Duller, G.A.T., Wintle, A.G., 1991. On infrared stimulated luminescence at elevated temperatures. Nucl. Tracks Radiat. Meas. 18, 379–384.

Duller, G.A.T., Bøtter-Jensen, L., 1993. Luminescence from potassium feldspars stimulated by infrared and green light. Radiat. Prot. Dosim. 47, 683–688.

Fattahi, M., 2009. The effect of thermal stimulation on the far-red and orange-red IRSL signal of a French K-rich feldspar: preliminary results. Geochronometria 34, 15–24.

Halperin, A., Braner, A.A., 1960. Evaluation of thermal activation energies from glow curves. Phys. Rev. 117, 408–415.

Hütt, G., Jaek, I., Tchonka, J., 1988. Optical dating: K-feldspars optical response stimulation spectra. Quarter. Sci. Rev. 7, 381–385.

Jain, M., Murray, A.S., Bøtter-Jensen, L., Wintle, A.G., 2005. A single-aliquot regenenerative-dose method based on IR (1.49eV) bleaching of the fast OSL component in quartz. Radiat. Meas. 39, 309–318.

Kitis, G., Kiyak, N.G., Polymeris, G.S., Pagonis, V., 2010. Investigation of OSL signals from very deep traps in unfired and fired quartz samples. Nucl. Inst. Meth. Phys. Res. B 268, 592–598.

Markey, B.G., Colyott, L.E., McKeever, S.W.S., 1995. Time-resolved optically stimulated luminescence from α-Al_2O_3:C. Radiat. Meas. 24, 457–463.

Markey, B.G., McKeever, S.W.S., Akselrod, M.S., Bøtter-Jensen, L., 1996. The temperature dependence of optically stimulated luminescence from α-Al_2O_3:C. Radiat. Prot. Dosim. 65, 185–189.

McKeever, S.W.S., Bøtter-Jensen, L., Agersnap Larsen, N., Duller, G.A.T., 1997. Temperature dependence of OSL curves: experimental and theoretical aspects. Radiat. Meas. 27, 161–170.

McKeever, S.W.S., Blair, M.W., Yukihara, E.G., DeWitt, R., 2010. The effect of low ambient temperatures on optically stimulated luminescence (OSL) processes: relevance to OSL dating of martian sediments. Radiat. Meas. 45, 60–70.

Mishra, D.R., Soni, A., Rawat, N.S., Kulkarni, M.S., Bhatt, B.C., Sharma, D.N., 2011. Method of measuring thermal assistance energy associated with OSL traps in α-Al_2O_3:C phosphor. Radiat. Meas. 46, 635–642.

Oster, L., Haddad, J., 2003. Kinetic modeling of the photo-stimulated exoelectron emission. Phys. Stat. Sol.(a) 196, 471–476.

Polymeris, G.S., Raptis, S., Afouxenidis, D., Tsirliganis, N.C., Kitis, G., 2010. Thermally assisted OSL from deep traps in Al_2O_3:C. Radiat. Meas. 45, 519–522.

Poolton, N.R.J., Bøtter-Jensen, L., Ypma, P.J.M., Johnsen, O., 1994. Influence of crystal structure on the optically stimulated luminescence properties of feldspars. Radiat. Meas. 23, 551–554.

Poolton, N.R.J., Bøtter-Jensen, L., Johnsen, O., 1995. Thermo-optical properties of optically stimulated luminescence in feldspars. Radiat. Meas. 24, 531–534.

Smith, B.W., Rhodes, E.J., 1994. Charge movements in quartz and their relevance to optical dating. Radiat. Meas. 23, 329–333.

Spooner, N.A., 1994. The optical dating signal from quartz. Radiat. Meas. 23, 593–600.